International Journal of Thermal Sciences 48 (2009) 1213–1222

Contents lists available at ScienceDirect

International Journal of Thermal Sciences

www.elsevier.com/locate/ijts

Accurate analytical models for fractional pressure rise in constant volume combustion

C.C.M. Luijten *, E. Doosje, L.P.H. de Goey

Eindhoven University of Technology, Department of Mechanical Engineering, PO Box 513, 5600 MB Eindhoven, The Netherlands

ARTICLE INFO

Article history:
Received 12 October 2007
Received in revised form 16 October 2008
Accepted 23 December 2008
Available online 21 January 2009

Keywords:
Explosion
Laminar burning velocity
Constant volume combustion
Cubic root law
Two-zone model
Multi-zone model

ABSTRACT

Laminar burning velocities S_L can be obtained from the pressure history in a constant volume combustion experiment. In the analysis of results, the relation between pressure and mass fraction burnt, $x(p)$, is crucial. The linear $x(p)$ relation by Lewis and Von Elbe is still widely used. Yet, from their original work a more accurate relation for $x(p)$ can be derived, as is demonstrated in this paper ("extended LvE"). In this work we introduce a two zone model that can be treated analytically, resulting in an $x(p)$-relation identical to "extended LvE". We then extend our analytical approach to a multi-zone model, which is used to benchmark several other analytical $x(p)$ relations. Results of the two-zone model are very close to the multi-zone results. Reported deviations between S_L from bomb data and from other methods may be attributed to the limited accuracy of the linear $x(p)$ relation, as is illustrated for stoichiometric methane–air combustion. Notably, for small x our new relation gives a factor of γ_b/γ_u difference in S_L as compared to the linear one, which has long been assumed to be correct for small x. Our new $x(p)$ result also leads to a new expression for the explosion constant K_G in the cubic root law.

1. Introduction

Deflagration of a combustible mixture in a confined volume is one of the "classical" combustion experiments, with a history of more than a century [2]. In such a 'combustion bomb' experiment, the burning velocity S_L is obtained from the pressure trace $p(t)$, sometimes combined with a measurement of the flame front velocity. The relation between the pressure trace and the laminar burning velocity can be expressed as an ordinary differential equation for the pressure, containing S_L as a parameter. Fitting the solution to an experimental pressure trace provides values of S_L. In its general form, the differential equation contains the mass fraction burnt, denoted as x. To solve it, the functional dependence $x(p)$ must be known, obviating the importance of accurate $x(p)$ relations in obtaining accurate burning velocities.

In the following section, the extensive literature on this subject is reviewed. It appears that a linear $x(p)$ relation is still widely used, in spite of its recognized limited accuracy. Yet, the computational simplicity of using an analytical $x(p)$ expression remains appealing. This has led us to the present work, the core of which lies in Section 3. After a short resume of the differential equation for the pressure, analytical $x(p)$ relations are discussed. This includes the work of Lewis and Von Elbe, several other published models, and the two- and multi-zone models of the present work.

In Section 4 the impact of the choice of $x(p)$ relation on burning velocity values is discussed. Finally, the impact of our new $x(p)$ expression on the explosion constant K_G in the so-called Cubic Root Law is addressed. Conclusions and recommendations are summarized in Section 5.

2. Literature review

Lewis and Von Elbe (further denoted, for brevity, as LvE) described the essential physics of a spherically propagating flame in a confined vessel [3]. A linear $x(p)$ relation, first introduced in their famous text book [1], is still used a lot in evaluating laminar burning velocities [4–9].

Around 1960, much work on constant volume combustion was done by the South-African group around C.J. Rallis [10–12]. In a later review [13], Rallis and Garforth argue that the constant volume method by that time (1980) is the most reliable method of measuring burning velocities.

In the mid-seventies, the USA National Bureau of Mines published some often cited papers on combustion bomb research [14–17]. Just as the South-African group, their work concentrates on evaluating the burnt gas temperature T_b.

In 1976, Bradley and Mitcheson (abbreviated further as B&M) published a review paper in which they compare the linear $x(p)$ approximation to the results of a numerical multi-zone model [18]. Their numerical results appear to be quite close (but not identical) to the linear relation. In contrast, B&M cite Perlee et al. [16], who estimated the burnt density from a uniform isentropic com-

* Corresponding author. Tel.: +31 40 2475347; fax: +31 40 2433445.
E-mail address: c.c.m.luijten@tue.nl (C.C.M. Luijten).

1290-0729/$ – see front matter
doi:10.1016/j.ijthermalsci.2008.12.020

Nomenclature

A_b	surface area of burnt zone	m^2
c	specific heat capacity	$J\,kg^{-1}\,K^{-1}$
C	molar heat capacity	$J\,mol^{-1}\,K^{-1}$
e	specific internal energy	$J\,kg^{-1}$
E	total internal energy	J
f	function defined in Eq. (20)	
K	heat of reaction according to definition Ref. [1]	$J\,mol^{-1}$
K_G	explosion constant	$bar\,m\,s^{-1}$
m	mass	kg
M	molar mass	$kg\,mol^{-1}$
n	number of moles	mol
p	pressure	bar
r_f	radius of flame	m
R_0	universal gas constant	$J\,mol^{-1}\,K^{-1}$
R	specific gas constant	$J\,kg^{-1}\,K^{-1}$
$\mathcal{R}_v$	effective vessel radius	m
S_L	laminar burning velocity	$m\,s^{-1}$
s	entropy	$J\,kg^{-1}\,K^{-1}$
t	time	s
T	temperature	K
$\overline{T}$	mass-averaged temperature	K
V	volume	m^3
v	specific volume	$m^3\,kg^{-1}$
x	mass fraction burnt	
Y_F	mass fraction of fuel	

Greek symbols

Δe	isochoric heat of combustion per kg mixture	$J\,kg^{-1}$
Δh_F	enthalpy of combustion per kg fuel	$J\,kg^{-1}$
Δp	pressure difference	bar
Δu_F	isochoric heat of combustion per kg fuel	$J\,kg^{-1}$
γ	specific heat ratio	
ρ	density	$kg\,m^{-3}$
ξ	ratio of moles after/before reaction	

Subscripts

0	reference state (1 atmosphere, 298.15 K)
b	pertaining to burnt mixture
e	final (end) condition
f	pertaining to flame
i	initial condition
j	pertaining to jth zone
L	laminar
n	pertaining to nth time step
p	at constant pressure
u	pertaining to unburnt mixture
v	at constant volume

Superscripts

(j)	pertaining to jth time step
(n)	pertaining to nth time step

pression of the burnt gases, leading to $x(p)$ results differing significantly from their extended numerical model. This observation makes B&M state that "procedures based on an 'a priori' assumption of this linear equation are preferable to those based on assumptions on the value of ρ_b". As we will demonstrate in this work, the model of Perlee et al. [16] actually violates energy conservation. Therefore B&M favor the linear expression possibly for the wrong reasons.

In 1980 Metghalchi and Keck first published their two-zone model, in which the equations for conservation of mass and energy are simultaneously solved [19]. Both the unburnt and burnt mixtures are treated as spatially uniform in pressure, temperature and composition. In their 1982 paper [20], an extensive list of possibly disturbing effects on the analysis is quantitatively discussed: wall heat transfer, burnt gas temperature gradient, buoyant rise of the flame, charge stratification, wrinkling of the flame, spark energy input, and radiative heat loss. All these effects are concluded to be of limited significance (generally smaller than 1%). This conclusion underlines the relevance of simple analytical models. In later papers, the two-zone model is further employed [20–22], continuing to date with state-of-the-art experiments in a micro-gravity environment, ruling out disturbances due to buoyancy [23,24].

In a later paper from Metghalchi's group, Elia et al. [22] extend the two-zone model to include multiple zones. In this way, the temperature gradient in the burnt gas is taken into account. Recently, Saeed and Stone [25] also published a multi-zone model. They compare the resulting evolution of pressure versus mass fraction burnt with the linear approximation. For a stoichiometric methane–air mixture, the multi-zone $x(p)$ curve is found to lie slightly below the linear one. This result will be readdressed in Section 4.

Recently, Farrell et al. [26] used a two-zone model to obtain laminar burning velocities of 45 hydrocarbons. Stone et al. [24] compare a two-zone model with the linear $x(p)$ model and conclude that the observed difference was always smaller than 1.6% for the conditions evaluated. This leads them to advocate the linear relation, with the additional argument that "many authors have suggested improvements to this method, but there is rarely any theoretical justification for the complexities that are introduced". Exactly this theoretical justification will be provided in the present paper.

Obviously, analytical approaches have some clear advantages, as witnessed by the extensive use of the linear relation in recent literature. Avoiding computational effort is one of them; giving better insight is another. Of course, within the class of analytical models one should strive for the highest possible accuracy. We will demonstrate that the accuracy of obtained burning velocity values can be increased with respect to the linear approximation. This comes at the expense of only a marginal increase in complexity.

3. Combustion bomb theory

In this section first the differential equation relating the pressure trace to burning velocity is presented in its general form, containing $x(p)$ and its derivative. The second part of this section deals with the analytical varieties of $x(p)$. The same $x(p)$ relation is shown to follow from an analytical treatment of the two-zone model, as well as from closer inspection of the multi-zone model of Lewis and Von Elbe. Next, the analytical zone model is extended to multiple zones. In addition, some alternative approaches from literature are discussed within the present context.

3.1. Assumptions and basic relations

The following assumptions are very often made in the analysis of constant volume combustion: (1) the uniform unburnt gas is initially at rest; (2) the pressure remains spatially uniform during combustion; (3) total mass and volume of the vessel contents are conserved; (4) external heat input, heat losses and buoyancy are negligible; (5) the flame front is spherical and infinitely thin;

(6) the effect of flame stretch is negligible; (7) the unburnt gas is compressed isentropically; (8) there is no heat transfer between the zones.

Starting from the above assumptions, a differential equation for the pressure can be derived. The derivation is presented in Appendix A, and the result – which is for instance found already in Ref. [10] – is

$$\frac{\mathrm{d}p}{\mathrm{d}t} = \frac{3}{\mathcal{R}_v}\left(\frac{\mathrm{d}x}{\mathrm{d}p}\right)^{-1}\left[1-\left(\frac{p_i}{p}\right)^{1/\gamma_u}(1-x)\right]^{2/3}\left(\frac{p}{p_i}\right)^{1/\gamma_u} S_L. \tag{1}$$

In this equation, $\mathcal{R}_v$ is the effective radius of the vessel and $\gamma_u = c_{pu}/c_{vu}$, the isentropic exponent of the unburnt mixture. Both x and its derivative $\mathrm{d}x/\mathrm{d}p$ depend on pressure.

Besides the above assumptions, a few model-specific ones are often made. In zone-based models, the change of specific heats with temperature is often taken into account, just as the shifting chemical equilibrium with temperature. However, inclusion of these phenomena requires numerical methods. Therefore in our two- and multi-zone models in Sections 3.2.2 and 3.2.3, we assume that both burnt and unburnt mixtures are perfect gases (ideal gases with constant specific heats over the temperature ranges of interest) with constant composition. The quantitative impact of this assumption is discussed in a separate paper [27], in which we compare our analytical two-zone model to several numerical models.

3.2. Pressure versus mass fraction burnt

3.2.1. Lewis and Von Elbe

The most cited $x(p)$ relation in literature equates the burnt mass fraction to the fractional pressure rise:

$$x = \frac{p-p_i}{p_e-p_i}. \tag{2}$$

Although some authors cite Ref. [3] as the original source, actually *it is not*. Ref. [3] provides a different relation, which in the current symbols reads

$$x = 1 - \frac{R_0 T_i(p_e/p_i - p/p_i)}{R_0 T_u(\gamma_b-\gamma_u)/(\gamma_u-1)+(\gamma_b-1)K}. \tag{3}$$

R_0 is the universal gas constant. The parameter K is related to the molar reaction enthalpy, expressed in current symbols as

$$K = \xi C_{pb} T_b - C_{pu} T_u, \tag{4}$$

where ξ is the ratio of burnt to unburnt numbers of molecules. The burnt temperature T_b differs for consecutively burning annular shells; the original LvE model is essentially a multi-zone one.

Later in their book [1], they present a lengthy derivation to prove Eq. (3). In a final simplifying step in Ref. [1], which comes down to assuming that $T_u = T_i$ in the denominator of Eq. (3) irrespective of x, the linear relation (2) is obtained.

Although the parameter K has no straightforward interpretation in the present context, LvE show that it can be obtained in two ways, giving the same result in very good approximation. The first is computation from Eq. (4); the other is using Eq. (3) and considering the limiting case for $x = 0$, $p = p_i$. Rearranging (3) for $p = p_i$ (where $T_u = T_i$) gives

$$K = \frac{R_0 T_i}{\gamma_b - 1}\left(\frac{p_e}{p_i} - \frac{\gamma_b - 1}{\gamma_u - 1}\right). \tag{5}$$

However, what LvE did *not* notice, is that insertion of Eq. (5) into Eq. (3) directly yields an $x(p)$ relation without further approximations. The result is

$$x = \frac{p - p_i\left[\left(\frac{\gamma_b-1}{\gamma_u-1}\right) + \frac{T_u}{T_i}\left(\frac{\gamma_u-\gamma_b}{\gamma_u-1}\right)\right]}{p_e - p_i\left[\left(\frac{\gamma_b-1}{\gamma_u-1}\right) + \frac{T_u}{T_i}\left(\frac{\gamma_u-\gamma_b}{\gamma_u-1}\right)\right]}, \tag{6}$$

which has never been published as far as the current authors are aware of.

The linear relation (2) is equivalent to Eq. (3) when $\gamma_u = \gamma_b$. As a consequence, the linear approximation may be in error when γ_u and γ_b differ – which is always the case, due to differences in both composition and temperature. Nevertheless, because of its appealing simplicity and reasonable accuracy, the linear relation has been used a lot for obtaining laminar burning velocities.

Dahoe et al. [5] give a derivation similar to the above, but immediately start from the linear relation (2). Eq. (1) then turns into

$$\frac{\mathrm{d}p}{\mathrm{d}t} = \frac{3(p_e-p_i)}{\mathcal{R}_v}\left[1-\left(\frac{p_i}{p}\right)^{1/\gamma}\frac{p_e-p}{p_e-p_i}\right]^{2/3}\left(\frac{p}{p_i}\right)^{1/\gamma} S_L \tag{7}$$

which is attributed by Bradley and Mitcheson [18] to Benson and Burgoyne [28]. In the same paper [5] a three-zone model is presented, which takes into account the finite thickness of the flame. Later, Dahoe and De Goey present an improvement to the three-zone model [4], however its derivation still postulates a linear $x(p)$ relation.

Senecal and Beaulieu [6] use the same model as Dahoe et al. in order to obtain new values for the explosion constant K_G (see Section 4.3) for several gases. In recent years, also Skjold et al. [7], Frijters et al. [8] and again Dahoe [9] have employed the linear relation (2) to derive burning velocities.

3.2.2. Analytical two-zone model

In a two-zone model, both the burnt and unburnt zones have uniform temperatures and compositions. Conservation of specific volume v and internal energy e is expressed by

$$v_t = x v_b + (1-x) v_u, \tag{8}$$

$$e_t = x e_b + (1-x) e_u, \tag{9}$$

where the subscript t denotes 'total', hence $v_t = V/m_i$ and $e_t = E/m_i$ where E is the total internal energy. For ideal gases Eq. (8) can be written as

$$\frac{R_u T_i}{p_i} = x\frac{R_b T_b}{p} + (1-x)\frac{R_u T_u}{p}. \tag{10}$$

The internal energy for a perfect gas can be written as $e = e_0 + c_v(T - T_0)$, where e_0 is the chemical energy stored in the mixture at a reference temperature T_0. Without loss of generality we can write

$$e_u(T_u) = c_{vu}(T_u - T_0) + \Delta e, \tag{11}$$

$$e_b(T_b) = c_{vb}(T_b - T_0), \tag{12}$$

where $\Delta e = e_{0,u} - e_{0,b}$. Inserting Eqs. (11) and (12) into Eq. (9) and rearranging gives

$$T_b = T_0 + \frac{1}{x c_{vb}}\left[x\Delta e + c_{vu}(T_i - T_0) - (1-x)c_{vu}(T_u - T_0)\right]. \tag{13}$$

Now T_b can be eliminated from Eq. (10) resulting in

$$\frac{p}{p_i} = (1-x)\frac{T_u}{T_i} + \frac{R_b}{R_u}\left(x\frac{T_0}{T_i} + \frac{1}{c_{vb}T_i}\left[x\Delta e + c_{vu}(T_i - T_0) - (1-x)c_{vu}(T_u - T_0)\right]\right). \tag{14}$$

For the limiting case $x = 1$ at $p = p_e$, we have

$$\frac{p_e}{p_i} = \frac{R_b}{R_u}\left(\frac{T_0}{T_i} + \frac{1}{c_{vb}T_i}\left[\Delta e + c_{vu}(T_i - T_0)\right]\right). \tag{15}$$

Inserting this expression for p_e back into Eq. (14) gives

$$\frac{p}{p_i} = (1-x)\frac{T_u}{T_i} + x\frac{p_e}{p_i} + (1-x)\left[\frac{R_b}{R_u}\frac{c_{vu}}{c_{vb}}\frac{T_i - T_u}{T_i}\right]. \tag{16}$$

The term in square brackets can be rewritten as

$$\frac{R_b}{R_u}\frac{c_{vu}}{c_{vb}}\frac{T_i - T_u}{T_i} = \frac{\gamma_b - 1}{\gamma_u - 1}\left(1 - \frac{T_u}{T_i}\right). \tag{17}$$

Inserting into Eq. (16) and rearranging for x we obtain

$$x = \frac{p - p_i\left[\left(\frac{\gamma_b-1}{\gamma_u-1}\right) + \frac{T_u}{T_i}\left(\frac{\gamma_u-\gamma_b}{\gamma_u-1}\right)\right]}{p_e - p_i\left[\left(\frac{\gamma_b-1}{\gamma_u-1}\right) + \frac{T_u}{T_i}\left(\frac{\gamma_u-\gamma_b}{\gamma_u-1}\right)\right]}. \tag{18}$$

Eq. (18) is identical to Eq. (6). This is remarkable, since the latter was derived from a multi-zone approach, whereas Eq. (18) follows from a two-zone model with uniform T_b.

As a final step, the above result is written fully in terms of pressure using Eq. (A.6). For later use, the result is given in a more concise form:

$$x = \frac{p - p_i f(p)}{p_e - p_i f(p)}, \tag{19}$$

where

$$f(p) = \left(\frac{\gamma_b - 1}{\gamma_u - 1}\right) + \left(\frac{\gamma_u - \gamma_b}{\gamma_u - 1}\right)\left(\frac{p}{p_i}\right)^{(\gamma_u-1)/\gamma_u}. \tag{20}$$

Differentiation is straightforward, yielding

$$\frac{\mathrm{d}x}{\mathrm{d}p} = \frac{1 - p_i f'(p)}{p_e - p_i f(p)} + \frac{p_i f'(p)[p - p_i f(p)]}{[p_e - p_i f(p)]^2}, \tag{21}$$

where

$$p_i f'(p) = \left(\frac{\gamma_u - \gamma_b}{\gamma_u}\right)\left(\frac{p}{p_i}\right)^{-1/\gamma_u}. \tag{22}$$

Both x and $(\mathrm{d}x/\mathrm{d}p)$ can be inserted into the differential equation (1), resulting in a lengthy but analytical expression that is easily evaluated with the help of a computer, without the need for numerical solution. The end result is not written explicitly here for reasons of space.

3.2.3. Analytical multi-zone model

The above methodology can be extended to multiple zones. A "zone" in this context means a portion of the gas that burns during the pressure rise from $p_i + (j-1)\Delta p$ to $p_i + j\Delta p$, where j runs from 1 to n and $\Delta p = (p_e - p_i)/n$. As shown by Elia et al. [22], the governing equations in a multi-zone approach are:

$$v_t = \sum_{j=1}^{n-1} x_j v_{bj} + x_n v_{bn} + \left[1 - \sum_{j=1}^{n-1} x_j - x_n\right] v_u, \tag{23}$$

$$e_t = \sum_{j=1}^{n-1} x_j e_{bj} + x_n e_{bn} + \left[1 - \sum_{j=1}^{n-1} x_j - x_n\right] e_u. \tag{24}$$

We have neglected heat loss by conduction to the bomb wall, which is included by Elia et al. Furthermore, we let the labeling of shells arbitrarily start at $j = 1$ (instead of 0), which seems more intuitive. Shells are burning consecutively; at any time step, a shell with index n is just burning, whereas shells with lower indices have already burnt in previous steps. For this reason, the terms containing x_n are taken out of the summation in Eqs. (23) and (24). The total burnt fraction after time step n is given by

$$x = \sum_{j=1}^{n} x_j. \tag{25}$$

The shells, represented by the summations, are assumed to heat up due to isentropic compression once they have burnt. Hence, their temperature T_{bj} at the time the nth shell is burning, is given by:

$$T_{bj}^{(n)} = T_{bj}^{(j)}\left(\frac{p^{(n)}}{p^{(j)}}\right)^{(\gamma_b-1)/\gamma_b} \qquad (j < n), \tag{26}$$

where $T_{bj}^{(j)} \equiv T_{bj}$ is the temperature that shell j attained during combustion. Since the temperatures of and mass fractions contained in previously burnt shells are kept track of in this way, only the incremental mass fraction and burnt temperature of the nth shell need to be computed for each time step. These follow analytically from relations (23) and (24), as we will demonstrate.

Reusing Eqs. (11) and (12), conservation of energy reads

$$\begin{aligned} &c_{vu}(T_i - T_0) + \Delta e \\ &\quad = \sum_{j=1}^{n-1} x_j c_{vb}\left(T_{bj}^{(n)} - T_0\right) + x_n c_{vb}(T_{bn} - T_0) \\ &\qquad + \left[1 - \sum_{j=1}^{n-1} x_j - x_n\right]\left(c_{vu}(T_u - T_0) + \Delta e\right). \end{aligned} \tag{27}$$

This can be rearranged for T_{bn}, resulting in

$$\begin{aligned} T_{bn} = T_0 + \frac{1}{x_n c_{vb}}\Bigg\{ &c_{vu}(T_i - T_0) + \Delta e - \sum_{j=1}^{n-1} x_j c_{vb}\left(T_{bj}^{(n)} - T_0\right) \\ &- \left[1 - \sum_{j=1}^{n-1} x_j - x_n\right]\left(c_{vu}(T_u - T_0) + \Delta e\right)\Bigg\}. \end{aligned} \tag{28}$$

The law of volume conservation (23) can for ideal gases be written as

$$\frac{p}{p_i} = \left[1 - \sum_{j=1}^{n-1} x_j - x_n\right]\frac{T_u}{T_i} + \sum_{j=1}^{n-1} x_j \frac{R_b}{R_u}\frac{T_{bj}^{(n)}}{T_i} + x_n \frac{R_b}{R_u}\frac{T_{bn}}{T_i}. \tag{29}$$

The values of x_j and T_{bj} belonging to previously burnt shells are known. T_{bn} is substituted from Eq. (28), resulting in an equation linear in x_n. Solving for x_n we obtain

$$\begin{aligned} x_n = &\left[\frac{R_b}{R_u}\frac{T_0}{T_i} - \frac{T_u}{T_i} + \frac{R_b}{R_u}\frac{e_u(T_u)}{T_i c_{vb}}\right]^{-1} \\ &\times \Bigg\{\frac{p}{p_i} - \left(1 - \sum_{j=1}^{n-1} x_j\right)\frac{T_u}{T_i} - \sum_{j=1}^{n-1} x_j \frac{R_b}{R_u}\frac{T_{bj}^{(n)}}{T_i} \\ &- \frac{R_b}{R_u}\frac{1}{T_i c_{vb}}\Bigg[e_u(T_i) - \sum_{j=1}^{n-1} x_j e_b\left(T_{bj}^{(n)}\right) \\ &- \left(1 - \sum_{j=1}^{n-1} x_j\right) e_u(T_u)\Bigg]\Bigg\}, \end{aligned} \tag{30}$$

where e_u and e_b are defined by (11) and (12), the ratio T_u/T_i is obtained from (A.6), and the burnt temperatures $T_{bj}^{(n)}$ follow from (26). In principle, by substitution of these expressions, the result for x_n (and hence for x) could be written explicitly in pressure. In view of the complexity of the result, however, this does not bring any added value to the argument.

3.2.4. The South-African 'school'

Based on the same assumptions mentioned in Section 3.1, O'Donovan and Rallis [10] present an $x(p)$ relation that in the present symbols reads

$$x = \frac{p - p_i(T_u/T_i)}{p_e(\overline{T_b}/\overline{T_e}) - p_i(T_u/T_i)} = \frac{\overline{T_e}}{\overline{T_b}} \left\{ \frac{p - p_i(p/p_i)^{(\gamma_u-1)/\gamma_u}}{p_e - (\overline{T_e}/\overline{T_b})p_i(p/p_i)^{(\gamma_u-1)/\gamma_u}} \right\}. \quad (31)$$

$\overline{T_b}$ is the mass averaged burnt temperature during combustion, with end value $\overline{T_e}$. T_b is determined for every burnt shell from 3 consecutive increases. First its unburnt temperature is determined from adiabatic compression. Its burnt temperature is then obtained from energy conservation for the shell *at constant pressure*. Finally, the burnt shell is further compressed (and heated) adiabatically. There is one important difference with the multi-zone approach: the energy conservation law is not solved for the system as a whole, but for each individual shell, assuming constant pressure during combustion.

As a further simplification to their model, O'Donovan and Rallis assume that $\overline{T_e}$ and $\overline{T_b}$ are equal during the whole combustion period. In this case one finds

$$x = \frac{p - p_i(p/p_i)^{(\gamma_u-1)/\gamma_u}}{p_e - p_i(p/p_i)^{(\gamma_u-1)/\gamma_u}}. \quad (32)$$

This expression is equivalent to our equation (18) if $\gamma_b = 1$. This is compatible with the assumption that the (mass averaged) burnt temperature does not vary over time in this model. O'Donovan and Rallis agree that this is a severe simplification, and suggest to measure the burnt temperature at the center of the bomb $T_{b,c}$ immediately after the start of combustion to evaluated $\overline{T_e}/\overline{T_b}$. In their later review paper [13] this method is still promoted.

3.2.5. USA Bureau of Mines 'school'

Nagy et al. [14] assume isentropic compression of the *burnt* mixture as well, expressed by

$$T_b = T_e \left(\frac{p}{p_e} \right)^{(\gamma_b-1)/\gamma_b}. \quad (33)$$

As shown by Bradley and Mitcheson, Nagy et al. arrive at the following differential equation for the pressure:

$$\frac{\mathrm{d}p}{\mathrm{d}t} = \frac{3\gamma S_L p}{R} \cdot \frac{p_e^{2/3\gamma}}{p_i^{1/\gamma}} \left(p_e^{1/\gamma} - p_i^{1/\gamma} \right)^{1/3} \left[1 - (p_i/p)^{1/\gamma} \right]. \quad (34)$$

The underlying $x(p)$ expression is not given explicitly by the authors. However, it is derived in Appendix B, as Eq. (B.6) in order to show (later in Section 4) why this model does not give satisfactory results.

Inserting Eq. (B.6) with $\gamma_u = \gamma_b = \gamma$ into Eq. (1) yields Eq. (34). However, in the calculations presented in the next section we have used different values for γ_u and γ_b. Notice that Eq. (B.6) approaches the linear LvE result when both γ values approach unity.

4. Results and discussion

4.1. Comparison of $x(p)$ relations

We start with a comparison of the various analytical $x(p)$ relations, namely: the linear relation (2); the analytical two-zone result (19); Eq. (B.6), first used implicitly in Ref. [14] and further denoted as "Nagy"; and the analytical multi-zone expression (25), with x_j's from Eq. (30). Since Eq. (19) is identical to Eq. (3), the latter is not separately considered. Another variant relation is Eq. (32). Since it follows as a limiting case for $\gamma_b = 1$ from Eq. (19), this relation is not used in the comparison.

As an example we will use stoichiometric combustion of methane with air throughout this section. In this example case, the effect of flame stretch is expected to be very small. The pressure rise is related to the mass consumption speed rather than the burning velocity [29]. The mass consumption speed is effected by stretch and preferential diffusion through the modified Markstein number, which is proportional to $(Le - 1)$ according to $M^* \propto Ze(Le - 1)/2$, Ze being the Zeldovich number [30]. As the Lewis number of methane is very close to unity, this effect is negligible in the case of methane. Rahim et al. [31] also argue that flame stretch is unimportant for methane–air flames.

The evaluation needs the following parameters:

- Initial and final pressures p_i and p_e;
- specific heats c_{vu}, c_{vb};
- specific gas constants R_u, R_b (equivalently, molar masses M_u and M_b);
- isentropic coefficients γ_u and γ_b (these follow from the above);
- isochoric heat of combustion per unit of mass, $\Delta e = Y_F \Delta u_F$.

The initial pressure is taken 1 bar, the initial temperature T_i is 298 K. In accordance with the perfect gas assumption constant specific heats are used, evaluated from the Burcat Tables [32]. For the unburnt mixture, c_p and c_v are evaluated at T_i (since T_u increases from about 300 to about 500 K, the associated error is small), giving $c_{pu} = 1078\ \mathrm{J\,kg^{-1}\,K^{-1}}$ and $c_{vu} = 777\ \mathrm{J\,kg^{-1}\,K^{-1}}$. The burnt properties are evaluated at the mass-averaged end temperature T_e, which is obtained by iterating the relation

$$T_e = T_0 + \frac{c_{vu}(T_i - T_0) + \Delta e}{c_{vb}(T_e)} \quad (35)$$

several times. In about 4 iterations, T_e converges within 1 to 2526 K. The molar masses are obtained from the reaction equation of methane with air, assuming complete combustion. The specific heat ratios have values $\gamma_u = 1.39$ and $\gamma_b = 1.24$, with burnt specific heats $c_{pb} = 1539\ \mathrm{J\,kg^{-1}\,K^{-1}}$ and $c_{vb} = 1238\ \mathrm{J\,kg^{-1}\,K^{-1}}$. Knowing the mass-averaged end temperature and molar mass, the end pressure p_e following from the ideal gas law is 8.47 bar. In the multi-zone computations 20 zones are used.

Y_F is the mass fraction of fuel in the mixture. The heat of reaction for the mixture Δe is based on the isochoric heat of reaction of the fuel Δu_F. The isochoric and isobaric heating values are related via

$$Y_F \Delta u_F = Y_F \Delta h_F - R_0 T_0 \left[\frac{1}{M_b} - \frac{1}{M_u} \right], \quad (36)$$

where Δh_F is the enthalpy of combustion and T_0 the thermochemical reference temperature. It is readily shown that the last term is negligible: in our example case it vanishes since M_b equals M_u for methane combustion.

Fig. 1 shows results of the different models. To facilitate comparison, a dimensionless pressure $p_r = (p - p_i)/(p_e - p_i)$ is introduced, and subtracted from x to emphasize mutual differences. An important conclusion from this figure is that the two-zone and multi-zone models cannot be distinguished. This suggests that inclusion of the temperature gradient in the burnt mixture is less essential than might be expected based on its appreciable value (from our multi-zone computations discussed in Section 3.2.3 we find a temperature difference of about 800 K near the end of combustion [33], a value reported by others as well. This high range is a consequence of neglecting dissociation in the burnt gas. For a broader discussion, see Ref. [27]). Indeed, the position of the "zone-based" lines is found to be quantitatively the same as reported by Saeed and Stone [25] – a few percent below the linear model around $x = 0.5$ (see their Fig. 10, based on identical conditions). These authors employ a multi-zone model in which both the burnt temperature gradient and shifting chemical equilibrium are taken into account. This confirms that the latter two effects seem to affect $x(p)$ less than might be expected.

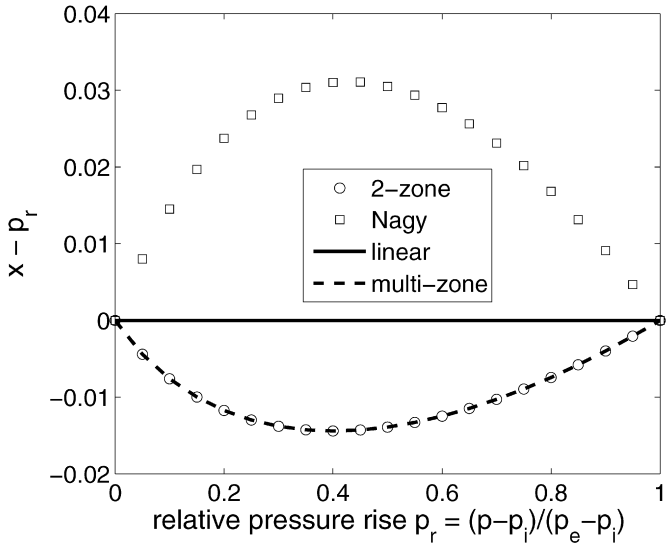

Fig. 1. Burnt mass fraction x as a function of relative pressure rise during stoichiometric combustion of methane with air, starting at $p_i = 1$ bar and $T_i = 298$ K. The linear model is subtracted to emphasize differences.

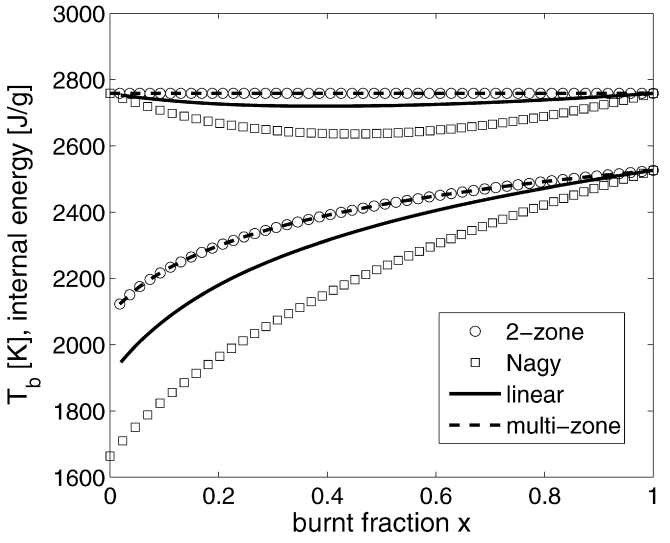

Fig. 2. Mass-averaged burnt temperature (lower curves) and total internal energy (upper curves) as a function of mass fraction burnt, same conditions as Fig. 1.

In contrast to the zone-based $x(p)$ curves, the Nagy result is above the linear result, and quantitatively deviates more. This observation was already made by Bradley and Mitcheson [18], comparing one of the relations of Perlee et al. [16] with the linear relation and their numerical multi-zone model.

In the remainder of this paper we will use the multi-zone model as a reference, because it captures most of the physics of the problem. The gradient in burnt temperature is covered, and conservation of energy is correctly solved for the system as a whole, in contrast to the local approximations applied in other models [1, 14]. This raises the question whether the other models would violate global conservation of energy. To answer this, the energy of the system is computed for each model. This requires knowledge of the (unburnt and) burnt temperatures. In the two-zone model T_b is solved directly. For the analytical multi-zone model the temperature distribution during combustion is kept track of. For the Nagy model, the burnt temperature follows from Eq. (33). Only for the Lewis and Von Elbe model, obtaining T_b is not straightforward. We shortcut this point by looking only at the mass-averaged burnt temperature $\overline{T_b}$. A general expression for $\overline{T_b}$ can be obtained (derived in Appendix C):

$$\overline{T_b} = T_i \frac{M_b}{M_u} \frac{p}{p_i} \frac{1}{x} \left[1 - (1-x) \left(\frac{p_i}{p} \right)^{1/\gamma_u} \right]. \tag{37}$$

Fig. 2 shows results of this relation for each model.

The internal energy of the system now follows using Eqs. (11) and (12). The results are also plotted in Fig. 2. By construction, the two-zone and multi-zone models obey conservation of energy. The small dip in the multi-zone curve near the end is an artifact of our labeling of zones, and can be made arbitrarily small by taking more zones (which does not really affect computation times since all relations are algebraic). The Nagy result is off by about 5% at maximum for these conditions. The linear relation is also off, albeit less (about 1.5%). Thus, these models both violate conservation of energy.

To interpret this result, it is good to realize that most *local* approximations of T_b were based on combustion at constant pressure. Locally over the flame front, energy conservation is solved at constant pressure. Hence, *isobaric* specific heat is used to obtain T_b. However, in the limit of only very few shells (especially in the limiting case of only one burning shell), the end temperature should obviously be based on the *isochoric* specific heat of the system. This contradiction apparently introduces an error in the local models for T_b, the magnitude of which depends on the number of zones taken into account. This can only be circumvented by the use of an integral formulation of energy conservation, as is done in the zone models.

This result can also be interpreted in terms of entropy. At intermediate stages of combustion, entropy increases more for the two-zone model than for the others, implying that the two-zone model carries the highest "degree of irreversibility" during the process. The two-step pathway as described in Appendix B apparently leads to erroneous results: forcing the burnt entropy to be constant artificially decreases the energy content of the system, according to the Second Law of Thermodynamics $T\,\mathrm{d}s \geqslant \mathrm{d}u$.

We conclude this subsection with an important comment on end pressures. We have taken p_e equal to 8.47 bar for all models, based on the assumptions of constant heat capacity and composition of the burnt mixture. The validity of these might be questioned. At higher temperatures some dissociation will occur, bringing about a change in heat capacity (which is in addition temperature dependent). We have compared our analytical two-zone model for the example case to an in-house numerical two-zone model, taking into account equilibrium chemistry and temperature dependent specific heats. Fig. 3 shows the results, plotted in the same fashion as Fig. 1. The main characteristics of the curves are similar, i.e. the largest deviation occurring at a relative pressure rise near 0.4, its value being close to 0.015. Apparently, the combined effect of dissociation and temperature dependent heat capacity is quite modest.

4.2. Laminar burning velocity

The most important consequence of the previous section lies in the determination of laminar burning velocities. Since the burning velocity is obtained by fitting experimental results to Eq. (1), we start with plotting results of that equation for a typical case, see Fig. 4. This solution is obtained using a standard Matlab solver routine (ode23). For this example we took the burning velocity S_L constant and equal to 0.4 $\mathrm{m\,s^{-1}}$ (approximately equal to the reported value for stoichiometric methane–air at atmospheric conditions).

The pressure in the two-zone model starts to rise earlier than in the other models. This can be understood from Eqs. (1) and

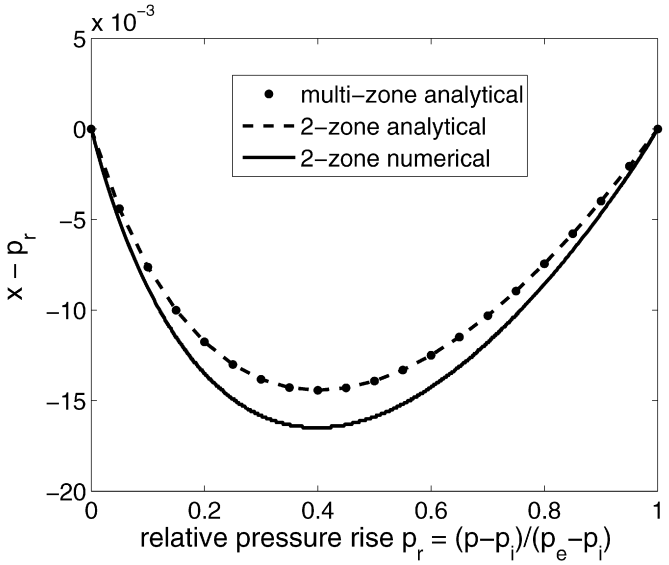

Fig. 3. Deviation of $x(p)$ from the linear relation for analytical and numerical models, same conditions as Fig. 1.

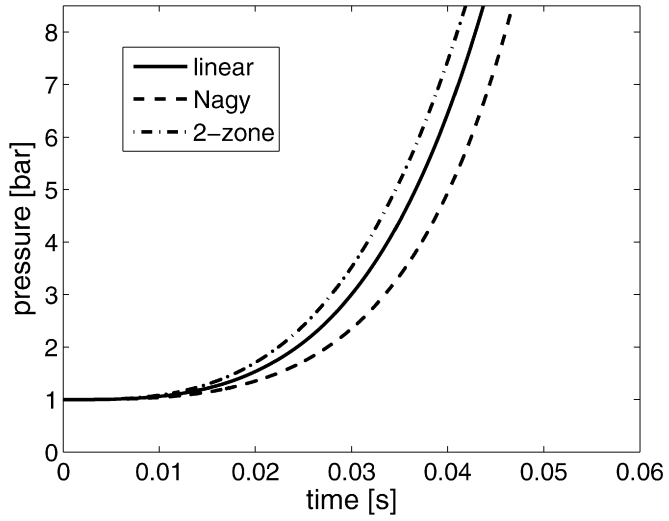

Fig. 4. Pressure as a function of time for stoichiometric combustion of methane–air, same conditions as Fig. 1. S_L is taken equal to 0.4 m s^{-1}.

(38): since for small x the derivative $\mathrm{d}x/\mathrm{d}p$ contains a factor γ_b/γ_u ($= 0.89$ for the present case) with respect to the linear model, the time derivative of pressure is larger for the two-zone model by a factor $1/0.89 = 1.12$. This result is confirmed by Bradley and Mitcheson [18].

Consequently, since burning velocity is obtained by 'scaling' the theoretical $p(t)$ curve to the experimental one, the linear model will give higher values of burning velocity for small x than the two-zone model. Although many authors have claimed that the linear relation would be correct for small x, actually *it is not*, as can already be seen from Fig. 1, where the slope of the zone-based curves deviates from unity already for small x. The error can be quantified using Eq. (22). The derivative for $x \to 0$ equals

$$\left(\frac{\mathrm{d}x}{\mathrm{d}p}\right)_{p=p_i} = \frac{(\gamma_b/\gamma_u)}{p_e - p_i}, \tag{38}$$

which for $\gamma_b \neq \gamma_u$ differs from the linear result by a factor (γ_b/γ_u).

The impact of using different $x(p)$ relations on laminar burning velocity over the full pressure range can be quantified as follows. Rearranging Eq. (1) gives

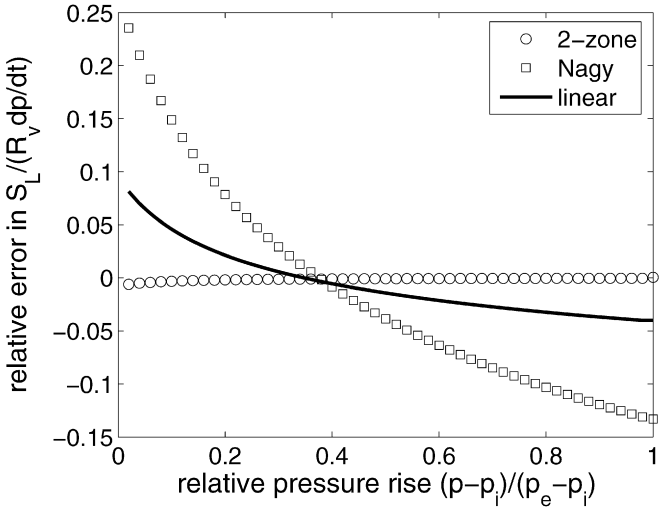

Fig. 5. Relative error of right-hand side of Eq. (39) with respect to the multi-zone results, same conditions as Fig. 1.

$$\frac{S_L}{\mathcal{R}_v(\mathrm{d}p/\mathrm{d}t)} = \frac{1}{3}\left(\frac{\mathrm{d}x}{\mathrm{d}p}\right)\left[1 - \left(\frac{p_i}{p}\right)^{1/\gamma_u}(1-x)\right]^{-2/3}\left(\frac{p}{p_i}\right)^{-1/\gamma_u}, \tag{39}$$

in which only the right-hand side depends on the $x(p)$ model used. Fig. 5 shows for each model the relative difference in the right-hand side of Eq. (39) with respect to the multi-zone model. Since the latter is believed to be the most accurate, this difference is named "error" in Fig. 5. This representation clearly shows that the obtained burning velocities $S_L(p,T)$, obtained from a certain pressure trace, significantly depend on the applied $x(p)$ model.

Again, the two-zone model is very close (within 1% for the present case) to the multi-zone results. This seems quite convincing evidence that inclusion of the burnt temperature gradient is less essential than intuition might say. The second important observation is that the linear $x(p)$ model for this case gives S_L results that are up to 8% too large in early stages of combustion, and down to 4% too small in late stages. Since many authors have applied the linear relation only to early stages of combustion (where it is erroneously believed to be correct, as demonstrated above) the error generally does not cancel.

We believe that the present results (certainly for a large part) explain the observations of Dahoe and De Goey [4], who reported burning velocities for stoichiometric methane–air that were larger than literature values by 5–10%.

Another important consequence of Fig. 5 is the following. In general, values of S_L are obtained over a range of pressures and temperatures by assuming a functional dependence $S_L(p,T)$ with two or more parameters (often powers of pressure and temperature). When fitting the resulting differential equation to an experimental pressure trace, the changing relative error observed in Fig. 5 will cause errors in the obtained exponents for the pressure and temperature dependence of S_L. We therefore believe that the present results should encourage anyone, who has used the linear relation to obtain burning velocities, to reinterpret their results using the more accurate $x(p)$ relation (19).

4.3. Explosion constant K_G in the Cubic Root Law

So far we have looked at burning velocities, and more in particular to the limiting case for small x. The other interesting limit is $x \to 1$. In practice this limit is often theoretical; usually the flame touches the vessel wall before $x = 1$. In the presence of heat loss the maximum rate of pressure rise occurs at an inflection point, with $x < 1$.

An explosion constant K_G is defined by

$$K_G \equiv \left(\frac{\mathrm{d}p}{\mathrm{d}t}\right)_{\max} V^{1/3}, \tag{40}$$

which is independent of the size of the vessel. With heat losses neglected, for the important limit of $x = 1$, Eq. (1) reduces to

$$\left(\frac{\mathrm{d}p}{\mathrm{d}t}\right)_{x\to 1} = \frac{3}{\mathcal{R}_v}\left(\frac{\mathrm{d}x}{\mathrm{d}p}\right)^{-1}_{x\to 1}\left(\frac{p_e}{p_i}\right)^{1/\gamma_u} S_L, \tag{41}$$

so that Eq. (40) can be written with $V = 4\pi\mathcal{R}_v^3/3$ as

$$K_G = (36\pi)^{1/3}\left(\frac{\mathrm{d}x}{\mathrm{d}p}\right)^{-1}_{p=p_e}\left(\frac{p_e}{p_i}\right)^{1/\gamma_u} S_L. \tag{42}$$

For the linear $x(p)$ model this results in

$$K_{G,\mathrm{linear}} = (36\pi)^{1/3}(p_e - p_i)\left(\frac{p_e}{p_i}\right)^{1/\gamma_u} S_L, \tag{43}$$

see for instance Ref. [5]. Likewise, the Nagy equation (B.6) gives

$$K_{G,\mathrm{Nagy}} = (36\pi)^{1/3}\gamma_b p_e\left[\left(\frac{p_e}{p_i}\right)^{1/\gamma_u} - 1\right] S_L. \tag{44}$$

For our equation (19) the maximum pressure derivative using Eq. (21) is

$$\left(\frac{\mathrm{d}x}{\mathrm{d}p}\right)_{p=p_e} = \frac{1}{p_e - p_i f(p_e)}. \tag{45}$$

Inserting this into Eq. (42) we arrive at

$$K_{G,2\mathrm{zone}} = (36\pi)^{1/3}\left[p_e - p_i f(p_e)\right]\left(\frac{p_e}{p_i}\right)^{1/\gamma_u} S_L, \tag{46}$$

where $f(p_e)$ is obtained from Eq. (20).

Recently, an alternative expression for K_G was published by Van den Bulck [34]. It is based on the two-zone model, which is however not solved in a completely algebraic manner. The author introduces an "apparent specific heat ratio" g_b, obtained from numerical computations. For K_G he finds

$$K_{G,\mathrm{VdB}} = (36\pi)^{1/3} g_b p_e\left[\left(\frac{p_e}{p_i}\right)^{1/\gamma_u} - 1\right] S_L. \tag{47}$$

Remarkably, this result is very similar to that based on Nagy's expression, the only difference being the appearance of g_b instead of γ_b.

Again a stoichiometric methane–air mixture is used as an example case, with parameter values as before. In Ref. [34] values of g_b are given for several fuel/air mixtures as a function of equivalence ratio. For stoichiometric methane–air, g_b is about 1.06. Using these input values and the above equations, one can compute that K_G/S_L (in bar) equals 168 for the linear model, 185 for the Nagy model, 161 for the two-zone model and 159 in the Van den Bulck model.

The linear model gives a value about 4% higher than the two-zone model. Van den Bulck [34] also reports that the linear approximation results in too high K_G, since it overestimates $\mathrm{d}p/\mathrm{d}x$ for x approaching unity. His expression gives a value very close to our two-zone one – in view of the accuracy of the value of 1.06 for g_b read from his graph, the values can be considered equivalent. This implies that, by "tuning" the value of g_b using a (numerically evaluated) two-zone model, quantitatively correct results are obtained. However, this needs to be redone for every condition, since the functional dependence of K_G in Eq. (47) is not correct, in view of the new two-zone based expression (46).

A remark is in place concerning the end pressure p_e. In all expressions in this work, its value should be based on the (theoretical) maximum value, assuming adiabatic combustion. In practice, heat losses will play a role towards the end of combustion, resulting in a lower experimental end pressure value; using it would introduce an error in S_L. For the same reason, the experimental maximum pressure rise rate will usually occur for $x < 1$. Hence, the experimental K_G is often not related to the experimental end pressure p_e. As already indicated, the K_G values obtained above shall be interpreted as theoretical upper limits, which are still very useful in safety engineering.

5. Conclusions

In obtaining laminar burning velocities from a constant volume combustion experiment, the relation between pressure p and mass fraction burnt x plays a crucial role. We have examined several analytical forms of this relation. The linear approximation, introduced by Lewis and Von Elbe, is still the most widespread analytical relation to interpret burning velocity data.

More recently two-zone models have been increasingly applied, although these have always been evaluated numerically. We have shown that it is possible to obtain an analytical $x(p)$ relation for the two-zone model, assuming perfect gas behavior for the burnt and unburnt mixtures, and neglecting dissociation. Remarkably, we were able to show that the same relation can be obtained from the early work of Lewis and Von Elbe, based on multiple zones. Examining the new expression, it appears that the linear approximation already deviates for small burnt fractions. Since the pressure derivative $\mathrm{d}x/\mathrm{d}p$ contains an extra factor γ_b/γ_u, burning velocities are obtained that are smaller than the linear result by the same factor. For the example case of a stoichiometric methane–air mixture, this factor is about 0.9.

We have extended our analytical $x(p)$ model to multiple zones. The resulting expressions in addition provide the temperature profile in the burnt mixture. Since this model captures most of the physics of the problem, its results were used as a benchmark for the other relations. Results of the two-zone model appear to be very close to the multi-zone result. Very importantly, this shows that inclusion of the temperature gradient of the burnt mixture only marginally affects $x(p)$ and thus burning velocities.

Some other classes of $x(p)$ relations that appeared earlier in literature have been included in the comparison. The models published by the USA Bureau of Mines were proven to violate integral energy conservation. The same holds for the linear approximation. Some other $x(p)$ relations from literature were shown to follow as limiting cases of our new equation (19).

Differences in laminar burning velocities between the varieties of $x(p)$ were quantified for the example case of stoichiometric methane–air combustion. We have demonstrated that reported deviations between burning velocities from bomb data and other methods can at least partly be ascribed to the limited accuracy of the linear approximation; for the example case, differences up to 8% were found. For this reason, we strongly suggest that S_L data, obtained from the constant volume method using the linear approximation, should be re-evaluated using the new expressions put forward in this paper.

Finally, our new $x(p)$ relation leads to a new expression for the explosion constant K_G in the "cubic root law", used to predict the maximal pressure rise upon explosion in a confined volume. For the example case, the new result was compared to K_G values based on the other models. Again, within the class of fully algebraic models, we believe that our new expression is the most correct.

Appendix A. Derivation of Eq. (1)

By definition of S_L we have

$$\rho_u A_b S_L = -\frac{\mathrm{d}m_u}{\mathrm{d}t}, \tag{A.1}$$

where A_b is the flame front surface area and ρ_u and m_u are the unburnt density and mass, respectively. Conservation of mass gives

$$-\frac{\mathrm{d}m_u}{\mathrm{d}t} = \frac{\mathrm{d}m_b}{\mathrm{d}t} = \rho_i V \frac{\mathrm{d}x}{\mathrm{d}t}, \tag{A.2}$$

where V is the vessel volume. The burnt mass fraction x is uniquely related to the pressure, so

$$\frac{\mathrm{d}x}{\mathrm{d}t} = \frac{\mathrm{d}x}{\mathrm{d}p} \times \frac{\mathrm{d}p}{\mathrm{d}t}. \tag{A.3}$$

Combining the above relations results in

$$\frac{\mathrm{d}p}{\mathrm{d}t} = \frac{A_b}{V}\frac{\rho_u}{\rho_i}\left(\frac{\mathrm{d}x}{\mathrm{d}p}\right)^{-1} S_L. \tag{A.4}$$

Isentropic compression of the unburnt mixture gives

$$\frac{\rho_u}{\rho_i} = \left(\frac{p}{p_i}\right)^{1/\gamma_u}, \tag{A.5}$$

or, alternatively,

$$T_u = T_i\left(\frac{p}{p_i}\right)^{(\gamma_u-1)/\gamma_u}. \tag{A.6}$$

Surface area and volume of the flame are related to its radius as $A_b = 4\pi r_f^2$ and $V_b = \frac{4}{3}\pi r_f^3$, respectively. Realizing that $m_u = \rho_i V(1-x)$, and $p_i = \rho_i R_u T_i$, the volume of the unburnt mixture can be written as

$$V_u = \frac{m_u R_u T_u}{p} = \frac{p_i}{p}\frac{T_u}{T_i}(1-x)V. \tag{A.7}$$

Inserting $V = \frac{4}{3}\pi\mathcal{R}_v^3$, where $\mathcal{R}_v$ is the effective radius of the vessel (which is not necessarily a sphere) and the above relations into $V = V_u + V_b$ yields

$$r_f = \mathcal{R}_v\left[1-(1-x)\frac{p_i}{p}\frac{T_u}{T_i}\right]^{1/3}. \tag{A.8}$$

The area-to-volume ratio in Eq. (A.4) now becomes

$$\frac{A_b}{V} = \frac{3}{\mathcal{R}_v}\left[1-(1-x)\frac{p_i}{p}\frac{T_u}{T_i}\right]^{2/3}. \tag{A.9}$$

Inserting Eqs. (A.5), (A.6) and (A.9) into Eq. (A.4) we finally obtain

$$\frac{\mathrm{d}p}{\mathrm{d}t} = \frac{3}{\mathcal{R}_v}\left(\frac{\mathrm{d}x}{\mathrm{d}p}\right)^{-1}\left[1-\left(\frac{p_i}{p}\right)^{1/\gamma_u}(1-x)\right]^{2/3}\left(\frac{p}{p_i}\right)^{1/\gamma_u} S_L. \tag{A.10}$$

Appendix B. Alternative derivation of Eq. (B.6)

During constant volume combustion, consider an intermediate situation where a fraction x has burnt; the total pressure p at that moment is uniform throughout the vessel. Thermodynamically, the pathway to this intermediate state might be constructed by considering two subsequent processes: first, burning of the fraction x at constant volume (which can be viewed of as a "thought experiment" in which an imaginary, temporary separation wall is built around a fraction x of the initial mixture), followed by pressure equilibration. In the first step, pressure and temperature of the burnt mixture rise at constant volume, whereas the unburnt mixture remains at the initial temperature and initial pressure p_i. In the second step, the unburnt mixture is compressed by the expanding burnt gases. Both expansion and compression are assumed to be adiabatic (no energy exchange other than compression work between burnt and unburnt mixture).

In the first step, the end temperature at constant volume, denoted as $\tilde{T}_b$, is obtained from the heat of reaction Δe and the (isochoric) specific heats c_v of the burnt and unburnt mixtures:

$$\tilde{T}_b = T_0 + \frac{1}{c_{vb}}\left[\Delta e + c_{vu}(T_i - T_0)\right]. \tag{B.1}$$

Note that $\tilde{T}_b$ does not depend on x, since both the amount of heat released and the total heat capacity of the burnt part scale linearly with x.

Using the same notation convention, we introduce $\tilde{V}_b$ for the volume after isochoric combustion. With total vessel volume V, it is obvious that $\tilde{V}_b = xV$. The pressure after isochoric combustion $\tilde{p}_b$ follows from the ideal gas law:

$$\tilde{p}_b = \frac{n_b R_0 \tilde{T}_b}{\tilde{V}_b} = \frac{\xi x n_0 R_0 \tilde{T}_b}{xV} = \frac{\xi n_i R_0 \tilde{T}_b}{V}. \tag{B.2}$$

This pressure does not depend on x, and therefore it also equals the end pressure p_e (at the end of combustion our "imaginary wall" is just the real wall of the vessel).

After isochoric combustion of the fraction x the imaginary wall is removed, allowing for pressure equilibration, which continues until the pressure is equal to p everywhere. The end volume of burnt mixture is denoted as V_b, which depends on x. For the burnt mixture we can write, using Poisson's law:

$$p_e(xV)^{\gamma_b} = pV_b^{\gamma_b}. \tag{B.3}$$

For the unburnt mixture we similarly have

$$p_i(V-xV)^{\gamma_u} = p(V-V_b)^{\gamma_u}. \tag{B.4}$$

Eqs. (B.3) and (B.4) are coupled equations for p and V_b for a given x. It is straightforward to eliminate $V_b(x)$, resulting in

$$p_i(1-x)^{\gamma_u} = p\left(1-x[p_e/p]^{1/\gamma_b}\right)^{\gamma_u}. \tag{B.5}$$

This equation is easily written explicitly in x, arriving at

$$x(p) = \frac{p^{1/\gamma_u} - p_i^{1/\gamma_u}}{p_e^{1/\gamma_b}p^{(1/\gamma_u - 1/\gamma_b)} - p_i^{1/\gamma_u}}. \tag{B.6}$$

Appendix C. Derivation of Eq. (37)

All models described in this work assume an infinitely thin flame front. In that case, the unburnt and burnt zones are clearly separated, which enables obtaining the mass-averaged temperature for the burnt zone as follows. The volumes of unburnt and burnt mixtures are

$$V_u = \frac{4}{3}\pi\left(\mathcal{R}_v^3 - r_f^3\right), \tag{C.1}$$

$$V_b = \frac{4}{3}\pi r_f^3. \tag{C.2}$$

With unburnt mass $m_u = (1-x)m_i$ and burnt mass $m_b = xm_i$, and using the ideal gas law, equality of pressures gives

$$\frac{(1-x)m_i(R_0/M_u)T_u}{\frac{4}{3}\pi(\mathcal{R}_v^3 - r_f^3)} = \frac{xm_i(R_0/M_b)\overline{T_b}}{\frac{4}{3}\pi r_f^3}, \tag{C.3}$$

which after rearrangement reads

$$\overline{T_b} = T_u\left(\frac{r_f^3}{\mathcal{R}_v^3 - r_f^3}\right)\frac{M_b}{M_u}\left(\frac{1-x}{x}\right). \tag{C.4}$$

Using Eq. (A.8) the factor containing radii can be rewritten as

$$\frac{r_f^3}{\mathcal{R}_v^3 - r_f^3} = \frac{1 - (1-x)\frac{p_i}{p}\frac{T_u}{T_i}}{(1-x)\frac{p_i}{p}\frac{T_u}{T_i}}, \tag{C.5}$$

insertion of which into (C.4) gives

$$\overline{T_b} = T_i \frac{p}{p_i}\frac{1}{x}\frac{M_b}{M_u}\left[1 - (1-x)\frac{p_i}{p}\frac{T_u}{T_i}\right]. \tag{C.6}$$

Finally, insertion of Eq. (A.6) gives the final result (37).

References

[1] B. Lewis, G. von Elbe, Combustion, Flames and Explosions of Gases, 2nd edition, Academic Press, New York, 1961.
[2] B. Hopkinson, Proc. Roy. Soc. A 77 (1906) 387.
[3] B. Lewis, G. von Elbe, Determination of the speed of flames and the temperature distribution in a spherical bomb from time-pressure explosion records, J. Chem. Phys. 2 (1934) 283–290.
[4] A. Dahoe, L. de Goey, On the determination of the laminar burning velocity from closed vessel gas explosions, J. Loss Prev. Process Ind. 16 (2003) 457–478.
[5] A. Dahoe, J. Zevenbergen, S. Lemkowitz, B. Scarlett, Dust explosions in spherical vessels: The role of flame thickness in the validity of the 'cube-root' law, J. Loss Prev. Process Ind. 9 (1) (1996) 33–44.
[6] J. Senecal, P. Beaulieu, K_g: New data and analysis, Process Safety Progress 17 (1) (1998) 9–15.
[7] T. Skjold, B. Arntzen, O. Hansen, O. Taraldset, I. Storvik, R. Eckhoff, Simulating dust explosions with the first version of DESC, Process Safety and Environmental Protection 83 (2005) 151–160.
[8] P. Frijters, R. Klein-Douwel, S. Manski, L. Somers, R. Baert, High speed analysis of high pressure combustion in a constant volume cell, in: J. Vandooren (Ed.), Proceedings of the European Combustion Meeting 2005, Louvain-la-Neuve, Belgium, 2005, paper 71.
[9] A. Dahoe, Laminar burning velocities of hydrogen–air mixtures from closed vessel gas explosions, J. Loss Prev. Process Ind. 18 (2005) 152–166.
[10] K. O'Donovan, C. Rallis, A modified analysis for the determination of the burning velocity of a gas mixture in a spherical constant volume combustion vessel, Combust. Flame 3 (1959) 201–214.
[11] C. Rallis, G. Tremeer, Equations for the determination of burning velocity in a spherical constant volume vessel, Combust. Flame 7 (1) (1963) 51–61.
[12] C. Rallis, A. Garforth, J. Steinz, Laminar burning velocity of acetylene–air mixtures by the constant volume method: Dependence on mixture composition, pressure and temperature, Combust. Flame 9 (4) (1965) 345–356.
[13] C. Rallis, A. Garforth, The determination of laminar burning velocity, Prog. Energy Combust. Sci. 6 (1980) 303–329.
[14] J. Nagy, J. Conn, H. Verakis, Explosion development in a spherical vessel, Tech. Rep. RI 7279, US Dept. of Interior, Bureau of Mines, 1969.
[15] J. Nagy, E. Seiler, J. Conn, H. Verakis, Explosion development in closed vessels, Tech. Rep. RI 7507, US Dept. of Interior, Bureau of Mines, 1971.
[16] H. Perlee, F. Fuller, C. Saul, Constant-volume flame propagation, Tech. Rep. RI 7839, US Dept. of Interior, Bureau of Mines, 1974.
[17] E. Kansa, H. Perlee, Constant volume flame propagation: Finite sound speed theory, Tech. Rep. RI 8163, US Dept. of Interior, Bureau of Mines, 1969.
[18] D. Bradley, A. Mitcheson, Mathematical solutions for explosions in spherical vessels, Combust. Flame 26 (1976) 201–217.
[19] M. Metghalchi, J. Keck, Laminar burning velocity of propane–air mixtures at high temperature and pressure, Combust. Flame 38 (1980) 143–154.
[20] M. Metghalchi, J. Keck, Burning velocities of mixtures of air with methanol, isooctane, and indolene at high pressure and temperature, Combust. Flame 48 (1982) 191–210.
[21] M. Ulinski, P. Moore, M. Elia, M. Metghalchi, Laminar burning velocity of methane–air–diluent mixtures, in: Proceedings of the ASME Internal Combustion Engine Division, vol. ICE 30-2, Fort Lauderdale, Florida, 1998.
[22] M. Elia, M. Ulinski, M. Metghalchi, Laminar burning velocity of methane–air–diluent mixtures, Trans. ASME 123 (2001) 190–196.
[23] M. Ulinski, Z. Li, M. Elia, C. Fletcher, M. Metghalchi, Burning velocity measurements in micro-gravity conditions, in: Proceedings of the 1999 Eastern Section of the Combustion Institute Meeting, Carolina State University, 1999.
[24] R. Stone, A. Clarke, P. Beckwith, Correlations for the laminar-burning velocity of methane/diluent/air mixtures obtained in free-fall experiments, Combust. Flame 114 (1998) 546–555.
[25] K. Saeed, C. Stone, The modelling of premixed laminar combustion in a closed vessel, Combust. Theory Modelling 8 (2004) 721–743.
[26] J. Farrell, R. Johnston, I. Androulakis, Molecular structure effects on laminar burning velocities at elevated temperature and pressure, SAE paper 2004-01-2936, 2004, pp. 11–32.
[27] C. Luijten, E. Doosje, J. van Oijen, L. de Goey, Impact of dissociation and end pressure on determination of laminar burning velocities in constant volume combustion, Int. J. Therm. Sci. 48 (2009) 1206–1212.
[28] R. Benson, J. Burgoyne, Report 76, British Shipbuilding Research Assoc., 1951.
[29] T. Poinsot, T. Echekki, M. Mungal, A study of the laminar flame tip and implications for premixed turbulent combustion, Combustion Science and Technology 81 (1) (1992) 45–73.
[30] L. de Goey, T. Plessing, R. Hermanns, N. Peters, Analysis of the flame thickness of turbulent flamelets in the thin reaction zones regime, Proc. Comb. Inst. 30 (2005) 859–866.
[31] F. Rahim, M. Elia, M. Ulinski, M. Metghalchi, Burning velocity measurements of methane-oxygen-argon mixtures and an application to extend methane–air burning velocity measurements, Int. J. Engine Research 3 (2) (2002) 81–92.
[32] A. Burcat, B. Ruscic, Ideal gas thermochemical database with updates from active thermochemical tables, http://garfield.chem.elte.hu/Burcat/burcat.html, 2007.
[33] C. Luijten, L. de Goey, New, accurate, analytical relations for fractional pressure rise, laminar burning velocity, and the cubic root law in constant volume combustion, in: G. Skevis (Ed.), Proc. 3rd European Combustion Meeting, 2007.
[34] E. Van den Bulck, Closed algebraic expressions for the adiabatic limit value of the explosion constant in closed volume combustion, J. Loss Prev. Process Ind. 18 (2005) 35–42.